Radio Science, Volume 14, Number 2, pages 253–268, March–April 1979

Pulsed electromagnetic radiation from a line source in a two-media configuration

A. T. de Hoop

Laboratory of Electromagnetic Research, Department of Electrical Engineering, Delft University of Technology, Delft, The Netherlands

(Received September 21, 1978.)

The pulsed electromagnetic radiation from a two-dimensional line source in a lossless two-media configuration is investigated theoretically. The author's modification of Cagniard's technique is used to derive closed-form expressions for the electromagnetic field components anywhere in the configuration. Numerical results are presented pertaining to the incident, the reflected, and the transmitted wave for different positions of the source and the observer, as well as for different contrasts of the two media. Also, the corresponding total-field plots are shown. In an appendix, the modified Cagniard contours pertaining to a lossless N-media configuration are discussed and some two-media modified Cagniard contours are shown.

1. INTRODUCTION

With the availability of sources of electromagnetic radiation that can generate pulses of very short duration, the demand arises for time-domain solutions of electromagnetic problems in certain idealized model situations. As far as the mathematical techniques are concerned, solutions of practical importance in a variety of cases can be obtained by applying a one-sided Laplace transform with respect to time and subjecting the resulting expressions for the relevant field quantities to an appropriate inversion technique. Of the latter, the Fast-Fourier-Transform technique and the Singularity Expansion Method [*Baum*, 1976*a*,*b*] are by now well known. For a number of configurations, however, an attractive alternative is furnished by the present author's modification of Cagniard's technique that has found wide application in the theory of seismic waves [*Cagniard*, 1939, 1962; *de Hoop*, 1958, 1960, 1961; *Achenbach*, 1973]. Also, a few electromagnetic problems have been investigated along these lines [*de Hoop and Frankena*, 1960; *Frankena*, 1960; *Langenberg*, 1974].

In the present paper, the modified Cagniard technique is used to calculate the electromagnetic field that is generated by a pulsed line source, located in one of two adjacent, nonconducting half spaces that show a finite contrast in their dielectric and magnetic properties. The attractiveness of the method lies in the fact that in our case (and in others as well) closed-form expressions are obtained for the electromagnetic field components in their dependence on position of observation and time. Expressions for the reflected field have been obtained before [*Felsen and Marcuvitz*, 1973], albeit in a slightly different form. The expressions for the transmitted field are of greater complexity and are, in their present form, believed to be new. If the speed of wave propagation in the source-free medium exceeds the speed of wave propagation in the medium in which the source is located, a lateral wave with a wedge-like wave front occurs in certain domains of observation. (In the frequency domain, the latter phenomenon corresponds to the occurrence of a totally-reflected wave.)

Numerical results are presented for a number of illustrative cases, as far as type of line source (electric or magnetic) and electromagnetic contrast of the two media are concerned.

In seismology, the modified Cagniard technique has been used in a variety of situations. The most complete solutions for the half-space problem have been reported by *Johnson* [1974]. He has computed, at an arbitrary point of observation, the particle displacement due to a concentrated force acting at an interior point of the medium. The most complicated terms in his expressions are the propagation factors that contain the two wave speeds of the isotropic solid. Appendix A of the present paper demonstrates that propagation factors containing N wave speeds ($N \geq 2$), such as occur in layered configurations, can be dealt with effec-

0048-6604/79/0304-0253$01.00

tively by employing a fast numerical routine that determines the proper modified Cagniard contours. The ingredients are: a numerical implementation of (A6) to obtain the arrival time of the relevant wave, followed by an iterative procedure that takes (A23) as a starting value for the body wave contour and (A24) as a starting value for the lateral wave (if present) contour; it is terminated as soon as (A3) is satisfied to the desired degree of accuracy. Our computations of the transmitted field (a case where $N = 2$) show that even the peculiar Cagniard contours shown in Figure 13 are computed in a few seconds on an IBM 370/158 computer.

At this point is may be remarked that, even before the work of *Johnson* [1974], authors considered special situations where only the Cagniard inversion of a propagation factor containing a single wave speed is required. These include: the surface displacement due to an interior source, the interior displacement due to a surface source, or the even simpler cases of epicentral displacements or surface displacements due to a surface source.

Application of the modified Cagniard technique to cases where anisotropic media are involved leads to difficulties of a different kind. These have been dealt with by *Burridge* [1971] and by *Suh et al.* [1974].

2. DESCRIPTION OF THE CONFIGURATION

We consider the electromagnetic field that is generated by a pulsed line source that is positioned parallel to the plane interface of two semi-infinite media occupying the half spaces D_1 and D_2. Their electromagnetic properties are described by a scalar, positive permittivity ε and a scalar, positive permeability μ. This implies that the two media are linear, homogeneous, isotropic, time-invariant, and lossless in their electromagnetic behavior. We let

$$\varepsilon = \varepsilon_1 \quad \text{and} \quad \mu = \mu_1 \quad \text{in } D_1 \tag{1}$$

$$\varepsilon = \varepsilon_2 \quad \text{and} \quad \mu = \mu_2 \quad \text{in } D_2 \tag{2}$$

To locate a point in the configuration, we employ the coordinates x, y, z with respect to a given orthogonal Cartesian reference frame that is specified by an origin O and three mutually perpendicular base vectors of unit length $\mathbf{i}_x$, $\mathbf{i}_y$, $\mathbf{i}_z$, that, in the given order, form a right-hand system. The reference frame is chosen such that

$$D_1: \quad -\infty < x < \infty, \quad -\infty < y < \infty, \quad -\infty < z < 0 \tag{3}$$

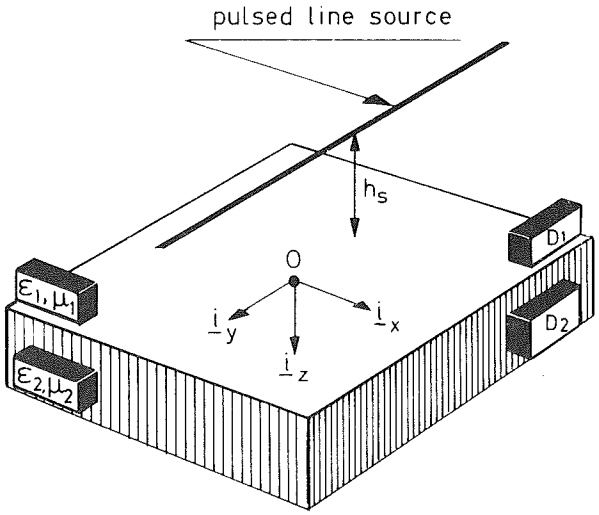

Fig. 1. Pulsed, electromagnetic line source in the presence of the plane boundary of two semi-infinite media.

$$D_2: \quad -\infty < x < \infty, \quad -\infty < y < \infty, \quad 0 < z < \infty \tag{4}$$

The time coordinate is denoted by t.

The configuration is excited by a line source that is located at $x = 0$, $-\infty < y < \infty$, $z = -h_s$, with $h_s > 0$. Hence, the source is located in D_1 and h_s is the distance from the line source to the interface of the two media. The source distribution is assumed to be independent of y. As a consequence, the entire electromagnetic field is two-dimensional and independent of y (Figure 1).

3. ELECTROMAGNETIC FIELD IN THE CONFIGURATION

The electromagnetic field in the configuration is described in terms of the electric field strength $\mathbf{E}$ and the magnetic field strength $\mathbf{H}$. The action of the source is characterized by specifying the volume densities of its electric current $\mathbf{J}$ and its magnetic current $\mathbb{K}$. In any domain where the field quantities are continuously differentiable, they satisfy the electromagnetic field equations (SI units are used throughout the paper):

$$\nabla \times \mathbf{H} = \varepsilon \partial_t \mathbf{E} + \mathbf{J} \tag{5}$$

$$\nabla \times \mathbf{E} = -\mu \partial_t \mathbf{H} - \mathbf{K} \tag{6}$$

$$\nabla \cdot (\varepsilon \partial_t \mathbf{E} + \mathbf{J}) = 0 \tag{7}$$

$$\nabla \cdot (\mu \partial_t \mathbf{H} + \mathbf{K}) = 0 \tag{8}$$

where partial differentiation is denoted by the

operator ∂. In accordance with the notation adopted in section 2, we write

$$\mathbf{E} = \mathbf{E}_1 \quad \text{and} \quad \mathbf{H} = \mathbf{H}_1 \quad \text{in } D_1 \tag{9}$$

$$\mathbf{E} = \mathbf{E}_2 \quad \text{and} \quad \mathbf{H} = \mathbf{H}_2 \quad \text{in } D_2 \tag{10}$$

Outside the source, that is located in D_1, we have $\mathbf{J} = \mathbf{0}$ and $\mathbf{K} = \mathbf{0}$. Across the interface of the two media, the boundary conditions

$$\lim_{z \uparrow 0} \{E_{1,x}, E_{1,y}, H_{1,x}, H_{1,y}\} = \lim_{z \downarrow 0} \{E_{2,x}, E_{2,y}, H_{2,x}, H_{2,y}\} \quad \text{for all } x \text{ and } y \tag{11}$$

hold. Further, the primary field, i.e., the field generated by the source, should travel away from the source and the secondary field, i.e., the field generated by the secondary sources at the interface, should travel away from the interface (radiation condition). In media of the type under consideration, electromagnetic waves travel at the speed

$$c = (\varepsilon\mu)^{-1/2} \tag{12}$$

where

$$c = c_1 \quad \text{in } D_1 \tag{13}$$

$$c = c_2 \quad \text{in } D_2 \tag{14}$$

We assume that the source starts to act at the instant $t = 0$. Prior to this instant, no electromagnetic field is assumed to be present in the configuration (initial condition).

In the course of the analysis, it is advantageous to introduce the three constituents that together form the total field. These are: (a) the incident field $\{\mathbf{E}^i, \mathbf{H}^i\}$, i.e., the field that the source would generate if no boundary were present; (b) the reflected field $\{\mathbf{E}^r, \mathbf{H}^r\}$, i.e., the difference between the total field in D_1 and the incident field: $\mathbf{E}^r = \mathbf{E}_1 - \mathbf{E}^i$, $\mathbf{H}^r = \mathbf{H}_1 - \mathbf{H}^i$; (c) the transmitted field $\{\mathbf{E}^t, \mathbf{H}^t\}$, which is nothing but another name for the total field in D_2: $\mathbf{E}^t = \mathbf{E}_2$, $\mathbf{H}^t = \mathbf{H}_2$. Each of these field constituents requires a separate treatment.

Next, we take into account the two-dimensionality of the problem. To this end, we decompose each vectorial quantity into a component parallel to the line source (this component is denoted by the subscript $\|$) and a component in the plane perpendicular to it (this component is denoted by the subscript $\perp$). For example, we write

$$\mathbf{E} = \mathbf{E}_\| + \mathbf{E}_\perp, \quad \text{etc.} \tag{15}$$

while

$$\nabla = \nabla_\perp \tag{16}$$

since $\nabla_\| = \mathbf{i}_y \partial_y = \mathbf{0}$. Substitution of (15) and (16) in (5)–(8) shows that as far as the electromagnetic field equations are concerned, two mutually uncoupled fields are generated, namely, an E-polarized field for which $\mathbf{E}_\| \neq \mathbf{0}$ and $\mathbf{H}_\| = \mathbf{0}$, and an H-polarized field for which $\mathbf{H}_\| \neq \mathbf{0}$ and $\mathbf{E}_\| = \mathbf{0}$. Since neither the boundary conditions nor the radiation condition nor the initial condition lead to coupling between the two types of polarization, the two types of field exist independently. In the final analysis, they will be discussed separately.

4. GENERAL STRUCTURE OF OUR FIELD REPRESENTATIONS

To carry out our analysis, we cast the field representations in a particular form that is characteristic of the modified Cagniard technique. First, we subject the field quantities to a one-sided Laplace transform with respect to time. One of the characteristic features of the Cagniard technique is that the relevant transform variable s is taken to be real and positive. Let us illustrate the procedure by considering the electric field strength. Denoting the Laplace transform of a quantity with respect to time by a circumflex over the relevant symbol, we have

$$\hat{\mathbf{E}}(x, z, s) = \int_0^\infty \exp(-st)\mathbf{E}(x, z, t)\,dt \tag{17}$$

We restrict a possible growth in time of the source strength to an exponential one at most and choose s so large that the right-hand side of (17) exists. Next, we subject the thus-transformed quantities to a Fourier transform with respect to the "horizontal" coordinate x. To avoid, however, the introduction of symbols that are not needed in the final evaluation of the expressions, we write this Fourier transform as a two-sided Laplace transform [*Van der Pol and Bremmer*, 1950], the transform variable p of which is purely imaginary. The quantity thus transformed is denoted by a tilde over the relevant symbol:

$$\tilde{\hat{\mathbf{E}}}(p, z, s) = \int_{-\infty}^\infty \exp(spx)\hat{\mathbf{E}}(x, z, s)\,dx \quad \text{with} \quad \mathrm{Re}(p) = 0 \tag{18}$$

The (real, positive) factor s in the exponential function is introduced here for later convenience. On account of Fourier's theorem, the inverse of (18) is

$$\hat{\mathbf{E}}(x, z, s) = (s/2\pi i) \int_{-i\infty}^{i\infty} \exp(-spx)\tilde{\mathbf{E}}(p, z, s)\mathrm{d}p \qquad (19)$$

Once $\tilde{\mathbf{E}}$ has been determined, the representation (19) is used to arrive at an expression for $\mathbf{E}(x, z, t)$. This is accomplished by a specific scheme of transformations in the complex p plane, followed by an application of the uniqueness theorem of the one-sided Laplace transform (17). Details of this procedure depend on the location of the singularities of $\tilde{\mathbf{E}}(p, z, s)$ in the complex p plane and the latter differ for the incident, the reflected, and the transmitted field. Therefore, the three field constituents will be discussed separately.

5. INCIDENT FIELD AND ITS REPRESENTATION

In this section we determine the representation of the type (19) for the incident field. This field satisfies (5)–(8), with $\varepsilon = \varepsilon_1$ and $\mu = \mu_1$ in the entire space. For the localized source of Figure 1 we have

$$\mathbf{J} = \mathbf{j}(t)\delta(x, z + h_s) \qquad (20)$$

$$\mathbf{K} = \mathbf{k}(t)\delta(x, z + h_s) \qquad (21)$$

After applying the transformations (17) and (18), we arrive at the expressions given below.

E-polarized field

$$\tilde{\mathbf{E}}^i_{\parallel} = [-\mu_1 \hat{\mathbf{j}}_{\parallel} - (-p\mathbf{i}_x \mp \gamma_1 \mathbf{i}_z) \times \hat{\mathbf{k}}_{\perp}](2\gamma_1)^{-1} \cdot \exp(-s\gamma_1|z + h_s|) \quad \text{when } z \gtrless -h_s \qquad (22)$$

$$\tilde{\mathbf{H}}^i_{\perp} = [(-p\mathbf{i}_x \mp \gamma_1 \mathbf{i}_z) \times \hat{\mathbf{j}}_{\parallel} - \varepsilon_1 \hat{\mathbf{k}}_{\perp} + (\mu_1)^{-1}(-p\mathbf{i}_x \mp \gamma_1 \mathbf{i}_z) \cdot \{(-p\mathbf{i}_x \mp \gamma_1 \mathbf{i}_z) \cdot \hat{\mathbf{k}}_{\perp}\}](2\gamma_1)^{-1} \exp(-s\gamma_1|z + h_s|) \quad \text{when } z \gtrless -h_s \qquad (23)$$

H-polarized field

$$\tilde{\mathbf{H}}^i_{\parallel} = [(-p\mathbf{i}_x \mp \gamma_1 \mathbf{i}_z) \times \hat{\mathbf{j}}_{\perp} - \varepsilon_1 \hat{\mathbf{k}}_{\parallel}](2\gamma_1)^{-1} \cdot \exp(-s\gamma_1|z + h_s|) \quad \text{when } z \gtrless -h_s \qquad (24)$$

$$\tilde{\mathbf{E}}^i_{\perp} = [-\mu_1 \hat{\mathbf{j}}_{\perp} + (\varepsilon_1)^{-1}(-p\mathbf{i}_x \mp \gamma_1 \mathbf{i}_z)\{(-p\mathbf{i}_x \mp \gamma_1 \mathbf{i}_z) \cdot \hat{\mathbf{j}}_{\perp}\} - (-p\mathbf{i}_x \mp \gamma_1 \mathbf{i}_z) \times \hat{\mathbf{k}}_{\parallel}](2\gamma_1)^{-1} \exp(-s\gamma_1|z + h_s|) \quad \text{when } z \gtrless -h_s \qquad (25)$$

in which

$$\gamma_1 = (1/c_1^2 - p^2)^{1/2} \quad \text{with } (\ldots)^{1/2} > 0 \quad \text{for } \mathrm{Re}(p) = 0 \qquad (26)$$

The choice of the square root, indicated in (26), ensures that the right-hand sides of (22)–(25) are bounded as $|z| \to \infty$, thus representing waves travelling away from the source.

6. REPRESENTATIONS FOR THE REFLECTED AND THE TRANSMITTED FIELD (*E*-POLARIZATION)

In this section we apply the transformations (17) and (18) to determine the representations of the type (19) for the reflected and the transmitted field that is E-polarized.

Reflected field. The reflected field is obtained as

$$\tilde{\mathbf{E}}^r_{\parallel} = R_E \tilde{\mathbf{E}}^i_{\parallel}(p, 0, s) \exp(s\gamma_1 z) \quad \text{with } -\infty < z < 0 \qquad (27)$$

$$\tilde{\mathbf{H}}^r_{\perp} = \mu_1^{-1}(p\mathbf{i}_x - \gamma_1 \mathbf{i}_z) \times \tilde{\mathbf{E}}^r_{\parallel} \quad \text{when } -\infty < z < 0 \qquad (28)$$

in which R_E denotes the electric field reflection factor for E-polarized waves and γ_1 is given by (26).

Transmitted field. The transmitted field is obtained as

$$\tilde{\mathbf{E}}^t_{\parallel} = T_E \tilde{\mathbf{E}}^i_{\parallel}(p, 0, s) \exp(-s\gamma_2 z) \quad \text{with } 0 < z < \infty \qquad (29)$$

$$\tilde{\mathbf{H}}^t_{\perp} = \mu_2^{-1}(p\mathbf{i}_x + \gamma_2 \mathbf{i}_z) \times \tilde{\mathbf{E}}^t_{\parallel} \quad \text{when } 0 < z < \infty \qquad (30)$$

in which T_E denotes the electric field transmission factor for E-polarized waves and γ_2 is given by

$$\gamma_2 = (1/c_2^2 - p^2)^{1/2} \quad \text{with } (\ldots)^{1/2} > 0 \quad \text{when } \mathrm{Re}(p) = 0 \qquad (31)$$

Applying the boundary conditions (cf. (11)), we obtain

$$R_E = (\gamma_1/\mu_1 - \gamma_2/\mu_2)/(\gamma_1/\mu_1 + \gamma_2/\mu_2) \qquad (32)$$

$$T_E = (2\gamma_1/\mu_1)/(\gamma_1/\mu_1 + \gamma_2/\mu_2) \qquad (33)$$

7. REPRESENTATIONS FOR THE REFLECTED AND THE TRANSMITTED FIELD (*H*-POLARIZATION)

In this section we apply the transformations (17) and (18) to determine the representations of the

type (19) for the reflected and the transmitted field that is H-polarized.

Reflected field. The reflected field is obtained as

$$\tilde{\mathbf{H}}^r_{\parallel} = R_H \tilde{\mathbf{H}}^i_{\parallel}(p, 0, s) \exp(s\gamma_1 z) \quad \text{with } -\infty < z < 0 \tag{34}$$

$$\tilde{\mathbf{E}}^r_{\perp} = -\varepsilon_1^{-1}(p\mathbf{i}_x - \gamma_1 \mathbf{i}_z) \times \tilde{\mathbf{H}}^r_{\parallel} \quad \text{when } -\infty < z < 0 \tag{35}$$

in which R_H denotes the magnetic field reflection factor for H-polarized waves and γ_1 is given by (26).

Transmitted field. The transmitted field is obtained as

$$\tilde{\mathbf{H}}^t_{\parallel} = T_H \tilde{\mathbf{H}}^i_{\parallel}(p, 0, s) \exp(-s\gamma_2 z) \quad \text{with } 0 < z < \infty \tag{36}$$

$$\tilde{\mathbf{E}}^t_{\perp} = -\varepsilon_2^{-1}(p\mathbf{i}_x + \gamma_2 \mathbf{i}_z) \times \tilde{\mathbf{H}}^t_{\parallel} \quad \text{when } 0 < z < \infty \tag{37}$$

in which T_H denotes the magnetic field transmission factor for H-polarized waves and γ_2 is given by (31). Applying the boundary conditions (cf. (11)), we obtain

$$R_H = (\gamma_1/\varepsilon_1 - \gamma_2/\varepsilon_2)/(\gamma_1/\varepsilon_1 + \gamma_2/\varepsilon_2) \tag{38}$$

$$T_H = (2\gamma_1/\varepsilon_1)/(\gamma_1/\varepsilon_1 + \gamma_2/\varepsilon_2) \tag{39}$$

8. MODIFIED CAGNIARD TECHNIQUE

In this section we outline the steps that will lead from the results of sections 5, 6, and 7 to the expressions for the field constituents in their dependence on position of observation and time. In their simplest form, the transformed field quantities show the following structure:

Incident field

$$\tilde{U}^i = \hat{f}(s) \exp(-s\gamma_1 |z + h_s|)/2\gamma_1 \quad \text{with } -\infty < z < \infty \tag{40}$$

Reflected field

$$\tilde{U}^r = \hat{f}(s) R \exp[-s\gamma_1(h_s - z)]/2\gamma_1 \quad \text{with } -\infty < z < 0 \tag{41}$$

Transmitted field

$$\tilde{U}^t = \hat{f}(s) T \exp[-s(\gamma_1 h_s + \gamma_2 z)]/2\gamma_1 \quad \text{with } 0 < z < \infty \tag{42}$$

In these expressions, U stands for one of the field components, $\hat{f}(s)$ stands for the Laplace transform of the source strength as a function of time, R is a reflection factor, and T is a transmission factor. Now it is important to observe that γ_1, γ_2 and R_E, T_E, R_H, T_H only contain p as transform variable, but not s. Consequently, the right-hand sides of (40)–(42) only contain s at the positions where this is indicated explicitly. Substituting the right-hand sides of (40)–(42) in representations of the type (19), we arrive at

$$\hat{U}^{i,r,t} = s\hat{f}(s) G^{i,r,t}(x, z, s) \tag{43}$$

in which

$$G^i = (2\pi i)^{-1} \int_{-i\infty}^{i\infty} \exp[-s(px + \gamma_1 |z + h_s|)](2\gamma_1)^{-1} \mathrm{d}p \tag{44}$$

$$G^r = (2\pi i)^{-1} \int_{-i\infty}^{i\infty} R \exp[-s\{px + \gamma_1(h_s - z)\}] \cdot (2\gamma_1)^{-1} \mathrm{d}p \tag{45}$$

$$G^t = (2\pi i)^{-1} \int_{-i\infty}^{i\infty} T \exp[-s(px + \gamma_1 h_s + \gamma_2 z)] \cdot (2\gamma_1)^{-1} \mathrm{d}p \tag{46}$$

The integrands in (44)–(46) admit analytic continuation into the complex p plane, away from the imaginary axis. The analytic continuation is taken such that $\mathrm{Re}(\gamma_1) \geq 0$ and $\mathrm{Re}(\gamma_2) \geq 0$ in the entire part of the p plane into which the path of integration is deformable. This implies that branch cuts are introduced at $\mathrm{Im}(p) = 0$, $1/c_1 < |\mathrm{Re}(p)| < \infty$, and at $\mathrm{Im}(p) = 0$, $1/c_2 < |\mathrm{Re}(p)| < \infty$.

It is easily verified that the reflection and transmission factors as defined by (32), (33), (38), and (39) contain no other singularities than the branch points $p = \pm 1/c_1$ and $p = \pm 1/c_2$; in particular, their denominators do not vanish in the cut p plane. By deforming, in the right-hand sides of (44)–(46), the original path of integration, $\mathrm{Re}(p) = 0$, into a so-called modified Cagniard contour (see Appendix A), the resulting expressions are all integrals of the general form

$$G = \int_{t_1}^{t_2} \exp(-s\tau) g(x, z, \tau) \mathrm{d}\tau \tag{47}$$

in which τ is a real variable of integration and t_1 and t_2 are non-negative. On account of the unique-

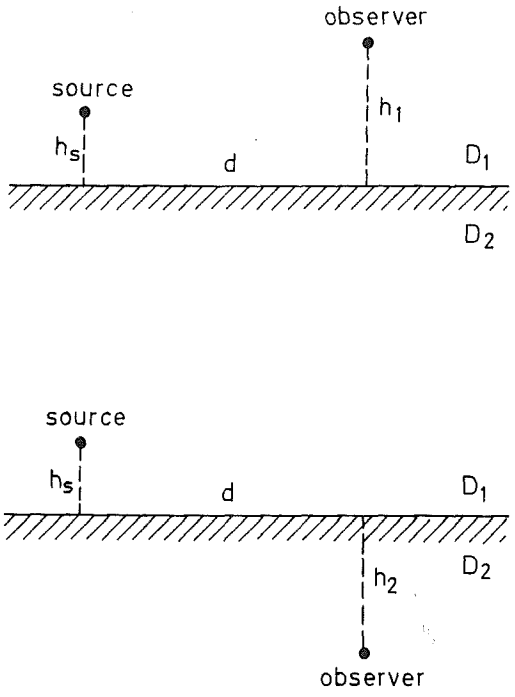

Fig. 2. Position of source and observer when observation takes place in D_1 and D_2, respectively.

ness of the one-sided Laplace transform with a real positive transform variable [*Widder*, 1946], (43) and (47) lead to

$$U = \begin{cases} 0, & \text{when } -\infty < t < t_1 \\ \displaystyle\int_{t_1}^{t} \partial_t f(t-\tau) g(x,z,\tau)\,\mathrm{d}\tau, & \text{when } t_1 < t < t_2 \\ \displaystyle\int_{t_1}^{t_2} \partial_t f(t-\tau) g(x,z,\tau)\,\mathrm{d}\tau, & \text{when } t_2 < t < \infty \end{cases} \tag{48}$$

where the convolution theorem and the differentiation rule of the Laplace transform have been used. From (48) it is clear that t_1 and t_2 can be identified with arrival times of wave fronts.

The modified Cagniard contours to be used in the representations of the incident, the reflected, and the transmitted wave are different and hence each of these field constituents will have a differently structured function g associated with it. Details of this will be given below. To facilitate the interpretation of the final results, the coordinates of the observer will be called $x = d$, $z = -h_1$, with $h_1 \geq 0$, when observation takes place in D_1, while the coordinates of the observer will be called $x = d$, $z = h_2$, with $h_2 \geq 0$, when observation takes place in D_2. Since the components of the field show either even or odd symmetry with respect to the plane $x = 0$ (the type of symmetry is easily inferred from the relevant formulas), we only consider non-negative values of d. Hence, d, h_1, and h_2, as well as h_s denote true distances (Figure 2).

9. NUMERICAL RESULTS

In this section we present some numerical results pertaining to the configuration shown in Figure 1. Before turning to the electromagnetic field components proper, we determine the time-domain expressions for g^i, g^r, and g^t that result from (44), (45), and (46), respectively.

Incident field. In the right-hand side of (44), the results pertaining to (A16) apply. Using (A23) we arrive at

$$g^i = \begin{cases} 0, & \text{when } -\infty < \tau < T^i \\ \dfrac{1}{2\pi(\tau^2 - T^{i2})^{1/2}} & \text{when } T^i < \tau < \infty \end{cases} \tag{49}$$

in which the arrival time T^i of the incident wave is given by

$$T^i = [d^2 + (h_1 - h_s)^2]^{1/2}/c_1 \tag{50}$$

The right-hand side of (49) is the fundamental wave shape of a two-dimensional, scalar (body) wave originating from a line source with unit-pulse time dependence. This wave shape is represented in Figure 3.

Reflected field. In all cases, the reflected field contains a body-wave contribution. To this part of the field, the results pertaining to (A16) apply, as (45) shows. Let θ_1 denote the angle introduced through

$$\sin(\theta_1) = d/[d^2 + (h_s + h_1)^2]^{1/2} \tag{51}$$

$$\cos(\theta_1) = (h_s + h_1)/[d^2 + (h_s + h_1)^2]^{1/2} \tag{52}$$

then application of (A23) to the right-hand side of (45) yields

$$g^{r,\mathrm{BW}} = \begin{cases} 0, & \text{when } -\infty < \tau < T^{r,\mathrm{BW}} \\ \dfrac{\mathrm{Re}\,[R(p^{r,\mathrm{BW}})]}{2\pi(\tau^2 - T^{r,\mathrm{BW}2})^{1/2}}, & \text{when } T^{r,\mathrm{BW}} < \tau < \infty \end{cases} \tag{53}$$

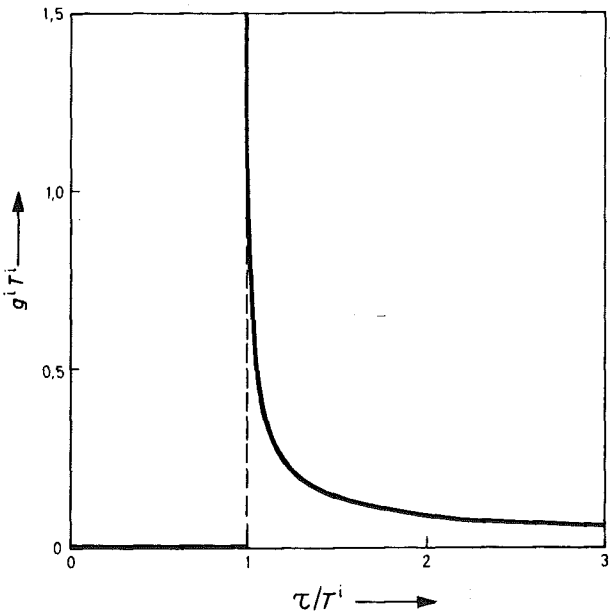

Fig. 3. Fundamental wave shape of a two-dimensional, scalar (body) wave originating from a line source with unit-pulse time dependence.

in which the arrival time $T^{r,BW}$ of the reflected body wave is given by (A23) and (A9):

$$T^{r,BW} = [d^2 + (h_s + h_1)^2]^{1/2}/c_1 = (h_s + h_1)/c_1 \cos(\theta_1) \tag{54}$$

and where (cf. (A23)):

$$p^{r,BW} = \frac{d}{d^2 + (h_s + h_1)^2}\tau + i\frac{h_s + h_1}{d^2 + (h_s + h_1)^2} \cdot \left[\tau^2 - \frac{d^2 + (h_s + h_1)^2}{c_1^2}\right]^{1/2} \quad \text{when } T^{r,BW} < \tau < \infty \tag{55}$$

In Figures 4 and 5 we have plotted some numerical values of the factor by which the fundamental wave shape, as occurring in (49) but with T^i replaced by $T^{r,BW}$, has to be multiplied to yield $g^{r,BW}$. The results marked "E-polarization" apply to the case $R = R_E$ (cf. (32)); the results marked "H-polarization" apply to the case $R = R_H$ (cf. (38)). Figure 4 illustrates the case $c_1 > c_2$; Figure 5 illustrates the case $c_1 < c_2$.

If $c_1 < c_2$, a lateral-wave contribution to the reflected wave occurs, in addition to the body-wave

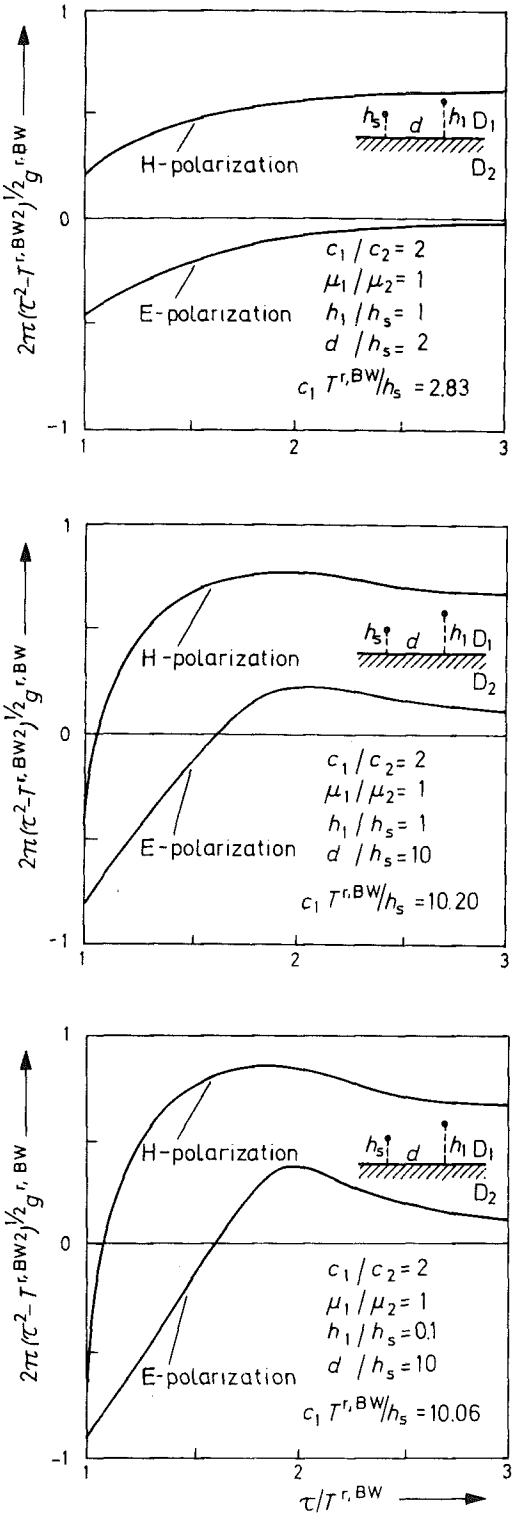

Fig. 4. The quantity $2\pi(\tau^2 - T^{r,BW2})^{1/2} g^{r,BW}$ as a function of $\tau/T^{r,BW}$ for different positions of observation ($c_1 > c_2$).

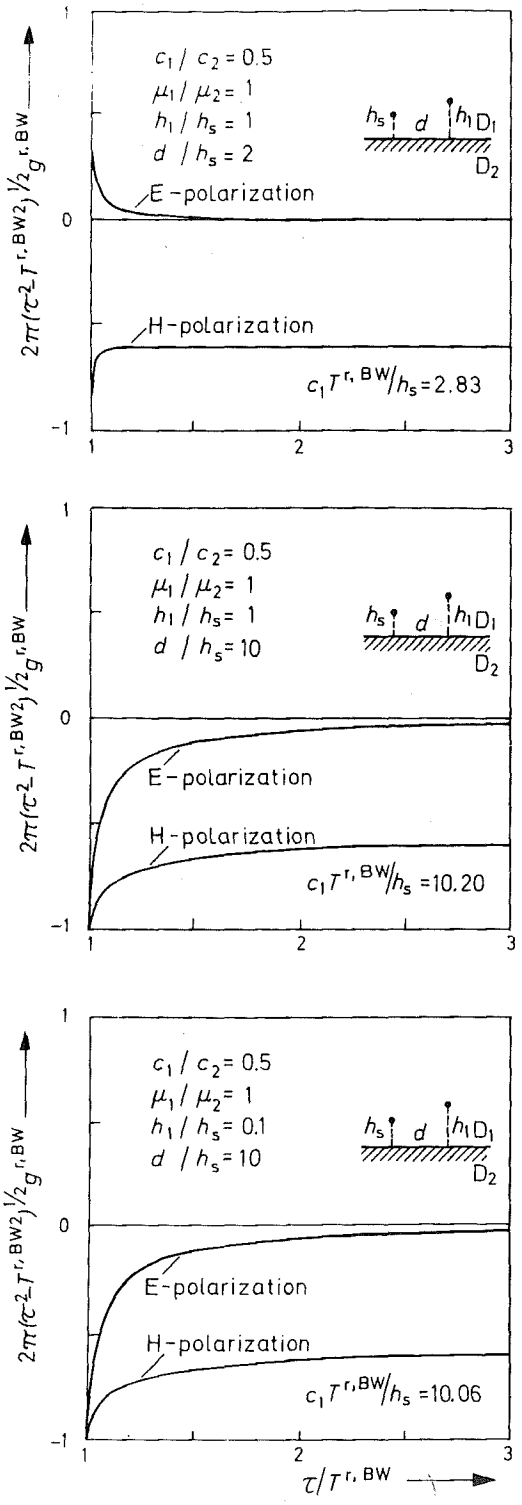

Fig. 5. The quantity $2\pi(\tau^2 - T^{r,BW2})^{1/2} g^{r,BW}$ as a function of $\tau/T^{r,BW}$ for different positions of observation ($c_1 < c_2$).

contribution, for those points of observation where $\sin(\theta_1) > c_1/c_2$. Application of (A24) to the right-hand side of (45) yields for this part of the field

$$g^{r,LW} = \begin{cases} 0, & \text{when } -\infty < \tau < T^{r,LW} \\ \dfrac{\text{Im}\,[R(p^{r,LW})]}{2\pi(T^{r,BW2} - \tau^2)^{1/2}}, & \\ & \text{when } T^{r,LW} < \tau < T^{r,BW} \\ 0, & \text{when } T^{r,BW} < \tau < \infty \end{cases} \tag{56}$$

in which the arrival time $T^{r,LW}$ of the reflected lateral wave is given by (cf. (A13)):

$$T^{r,LW} = d/c_2 + (1/c_1^2 - 1/c_2^2)^{1/2}(h_s + h_1) \tag{57}$$

while $T^{r,BW}$ is given by (54). Further, we have (cf. (A24)):

$$p^{r,LW} = \frac{d}{d^2 + (h_s + h_1)^2}\tau - \frac{h_s + h_1}{d^2 + (h_s + h_1)^2} \cdot \left[\frac{d^2 + (h_s + h_1)^2}{c_1^2} - \tau^2\right]^{1/2}$$

$$\text{when } T^{r,LW} < \tau < T^{r,BW} \tag{58}$$

In Figure 6 we have plotted some numerical values of the factor by which the fundamental wave shape, as occurring in (53) but with the role of observation time τ and arrival time of the reflected body wave $T^{r,BW}$ interchanged, has to be multiplied to yield $g^{r,LW}$. The results marked "E-polarization" apply to the case $R = R_E$ (cf. (32)); the results marked "H-polarization" apply to the case $R = R_H$ (cf. (38)).

Transmitted field. The transmitted field consists of a body wave only. Now, the results pertaining to (A3) apply with $N = 2$ as (46) shows. Let θ_1 and θ_2 denote the angles introduced through (cf. (A7)):

$$(1/c_1)\sin(\theta_1) = (1/c_2)\sin(\theta_2) \tag{59}$$

and

$$d - h_s\tan(\theta_1) - h_2\tan(\theta_2) = 0 \tag{60}$$

then, (46) leads to

$$g^t = \begin{cases} 0, & \text{when } -\infty < \tau < T^t \\ (2\pi)^{-1}\,\text{Im}\,[T(p^t)\gamma_1(p^t)^{-1}\partial_\tau p^t], & \\ & \text{when } T^t < \tau < \infty \end{cases} \tag{61}$$

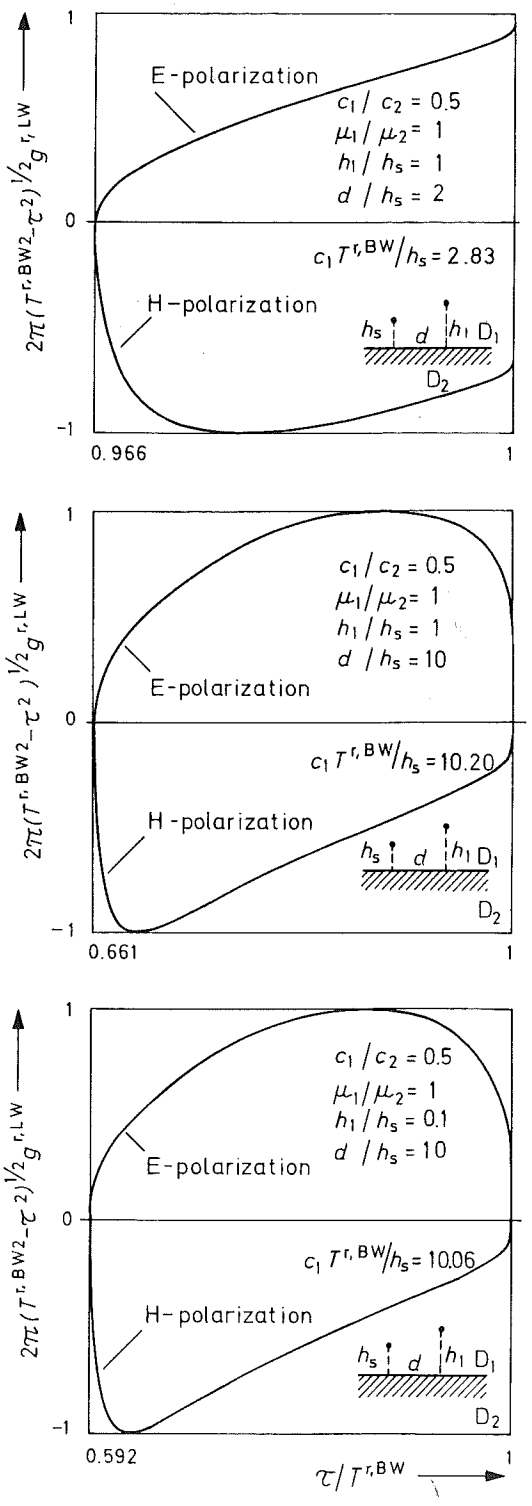

Fig. 6. The quantity $2\pi(T^{r,BW2} - \tau^2)^{1/2} g^{r,LW}$ as a function of $\tau/T^{r,BW}$ for different positions of observation in the domain $d/[d^2 + (h_s + h_1)^2]^{1/2} > c_1/c_2$ in the case $c_1 < c_2$.

in which the arrival time T^t of the transmitted wave is given by (cf. (A9)):

$$T^t = h_s/c_1 \cos(\theta_1) + h_2/c_2 \cos(\theta_2) \tag{62}$$

while $p = p^t$ is the part of the body-wave modified Cagniard contour that follows from

$$pd + \gamma_1 h_s + \gamma_2 h_2 = \tau \tag{63}$$

and is situated in the first quadrant of the complex p plane. In Figures 7 and 8 we have plotted some numerical values of the factor by which the fundamental wave shape, as occurring in (49) but with T^i replaced by T^t, has to be multiplied to yield g^t. The results marked "E-polarization" apply to the case $T = T_E$ (cf. (33)); the results marked "H-polarization" apply to the case $T = T_H$ (cf. (39)). Figure 7 illustrates the case $c_1 > c_2$; Figure 8 illustrates the case $c_1 < c_2$.

The results presented in Figures 4–8 can be used to construct plots of the electric (magnetic) field strength at a certain position of observation against time. A few examples are shown in Figures 9–11.

As electric current source strength we have taken

$$\mathbf{j}_\parallel = \begin{cases} \mathbf{0}, & \text{when } -\infty < t < 0 \\ I_0 \mathbf{i}_y, & \text{when } 0 < t < \infty \\ & \text{and hence } \hat{\mathbf{j}}_\parallel = (I_0/s)\mathbf{i}_y \end{cases} \tag{64}$$

As magnetic current source strength we have taken

$$\mathbf{k}_\parallel = \begin{cases} \mathbf{0}, & \text{when } -\infty < t < 0 \\ V_0 \mathbf{i}_y, & \text{when } 0 < t < \infty \\ & \text{and hence } \hat{\mathbf{k}}_\parallel = (V_0/s)\mathbf{i}_y \end{cases} \tag{65}$$

Hence, the fields shown are of a Green's function nature. For the media we have taken two (lossless) dielectrics. The results for other field components or for other types of excitation follow from the results of sections 5–7 and a subsequent application of the modified Cagniard technique. This involves not more than the inclusion of additional algebraic factors in the expressions to be evaluated along the modified Cagniard contours and—for time dependences that differ from (64) and (65)—the evaluation of the convolution integral (48). This convolution takes into account the actual pulse shape of the source. The frequency range of this pulse should be limited such that the idealization of lossless media is permitted.

The computations were performed on the IBM

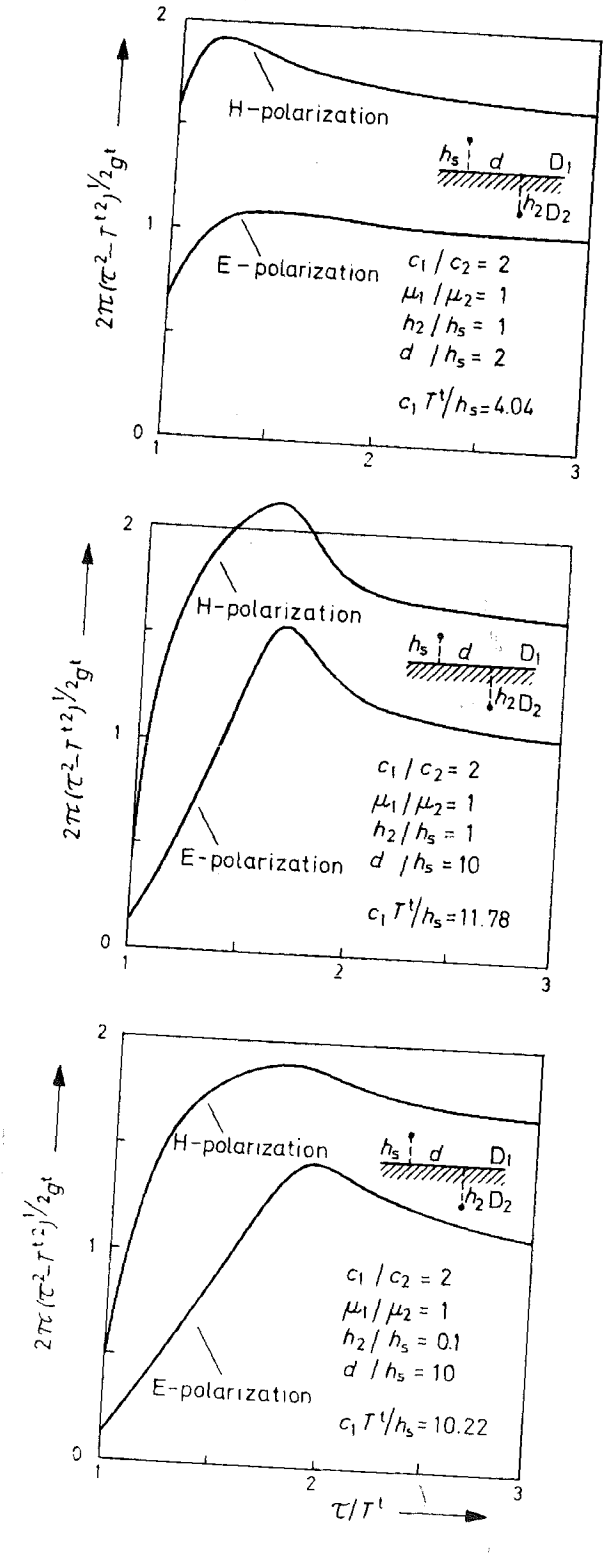

Fig. 7. The quantity $2\pi(\tau^2 - T'^2)^{1/2} g'$ as a function of τ / T' for different positions of observation ($c_1 > c_2$).

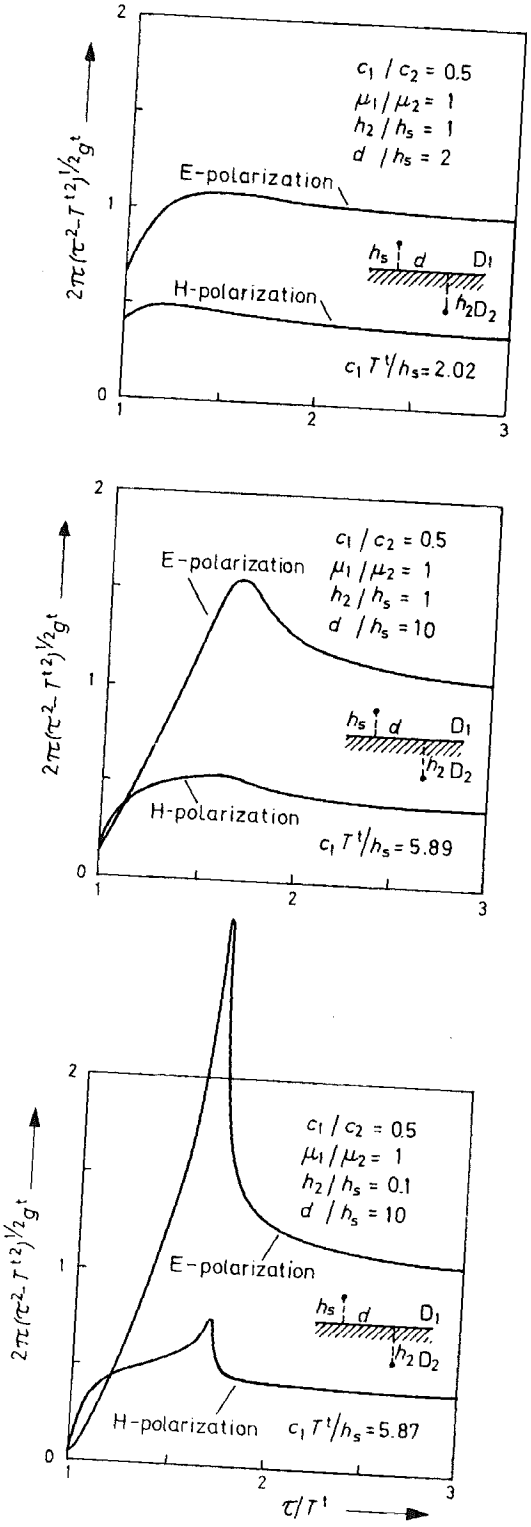

Fig. 8. The quantity $2\pi(\tau^2 - T'^2)^{1/2} g'$ as a function of τ / T' for different positions of observation ($c_1 < c_2$).

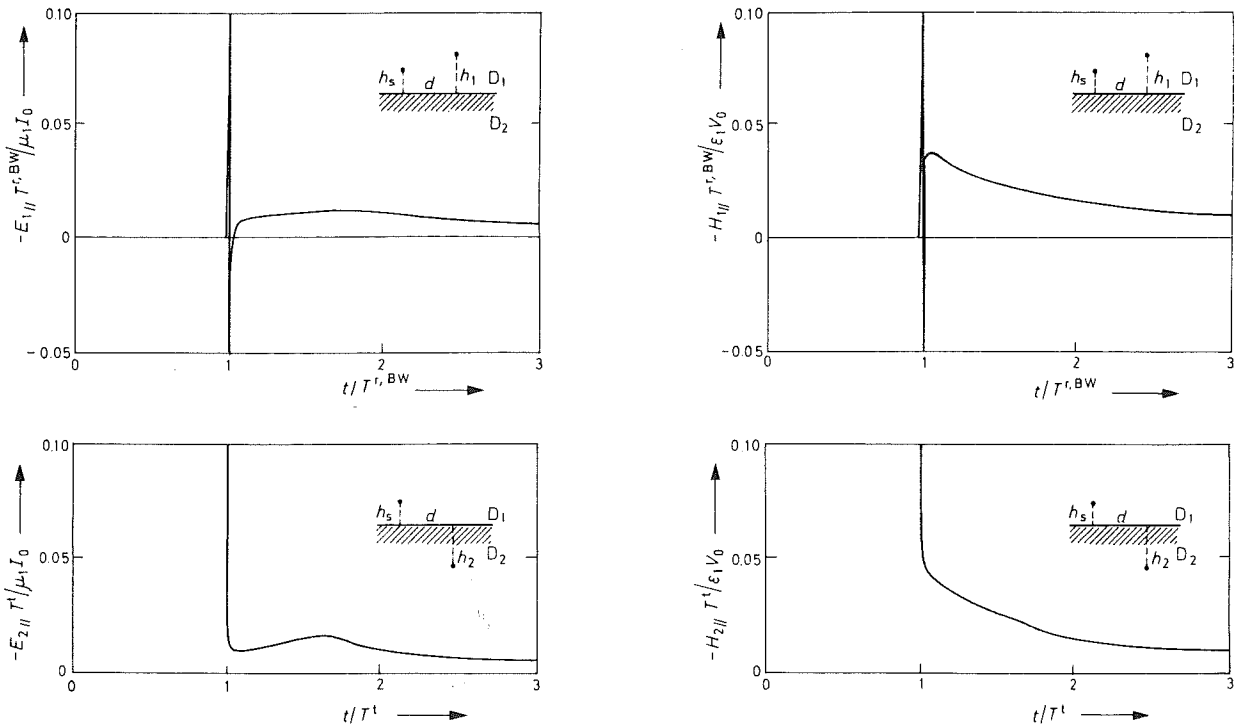

Fig. 9. Field from a pulsed line source in a two-media configuration ($c_1/c_2 = 2$, $\mu_1/\mu_2 = 1$, $h_1/h_s = 1$, $h_2/h_s = 1$, $d/h_s = 10$; $c_1 T^{r,BW}/h_s = 10.19$, $c_1 T^{t}/h_s = 11.8$).

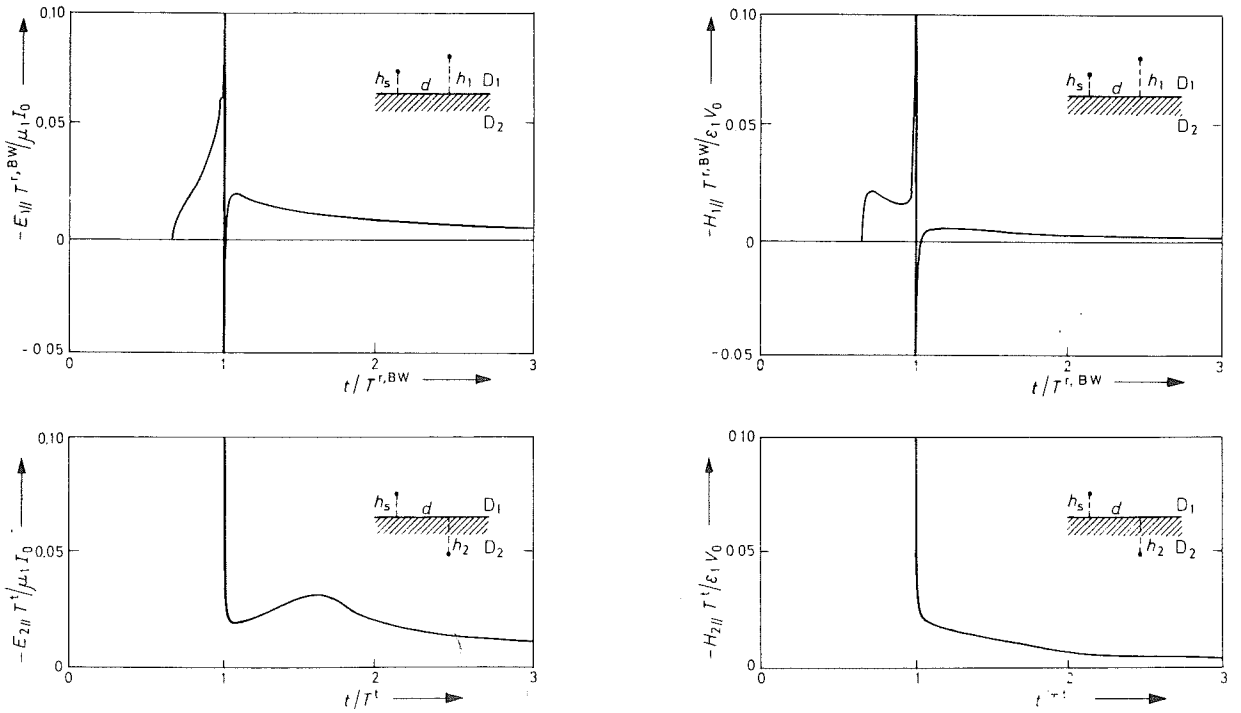

Fig. 10. Field from a pulsed line source in a two-media configuration ($c_1/c_2 = 0.5$, $\mu_1/\mu_2 = 1$, $h_1/h_s = 1$, $h_2/h_s = 1$, $d/h_s = 10$; $c_1 T^{r,BW}/h_s = 10.19$, $c_1 T^{t}/h_s = 5.89$).

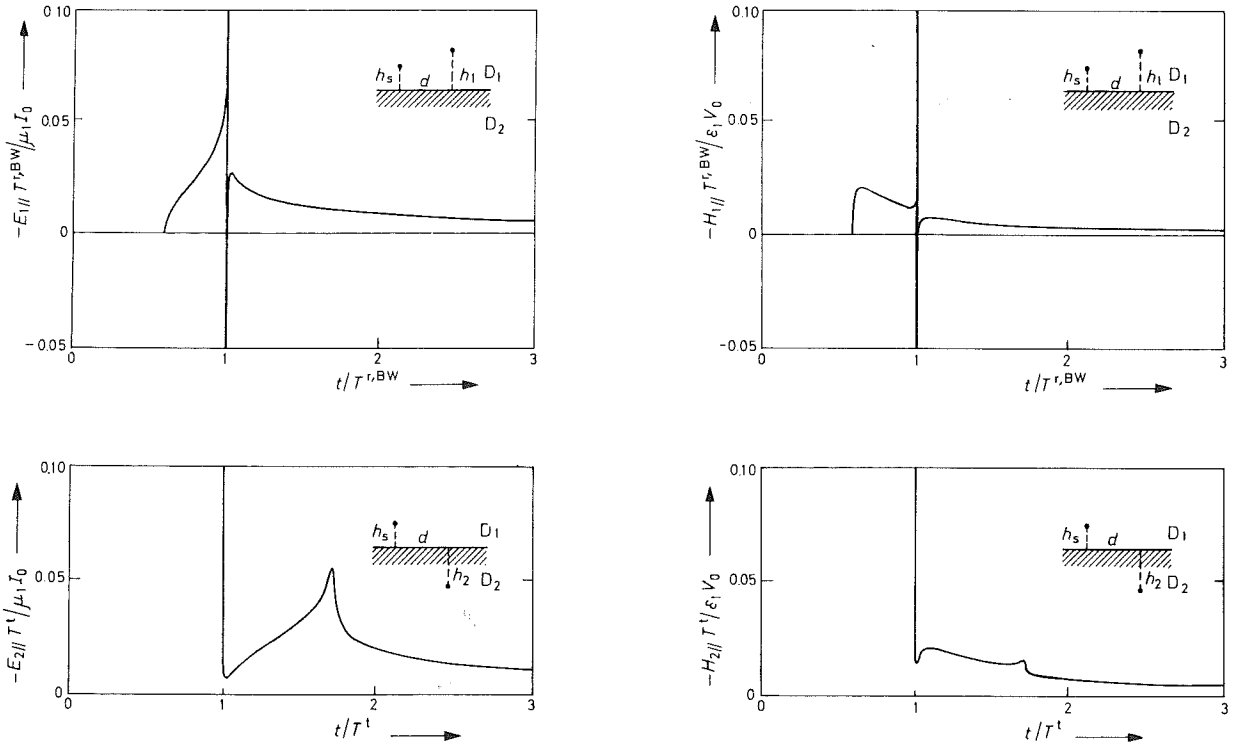

Fig. 11. Field from a pulsed line source in a two-media configuration ($c_1/c_2 = 0.5$, $\mu_1/\mu_2 = 1$, $h_1/h_s = 0.1$, $h_2/h_s = 0.1$, $d/h_s = 10$; $c_1 T^{r,BW}/h_s = 10.06$, $c_1 T^t/h_s = 5.87$).

370/158 computer of the Computing Center of the Delft University of Technology. The program was written in PL/I. Typical computation times for a single plot of the type shown in Figures 9–11 are 10 seconds.

APPENDIX A: SOME GENERAL PROPERTIES OF MODIFIED CAGNIARD CONTOURS

In this appendix we outline some general properties of modified Cagniard contours as they occur in problems associated with the propagation of pulsed waves in a layered configuration consisting of N different media ($N \geq 1$). The media occupy the domains $D_1, \ldots, D_N$, respectively. The modified Cagniard technique starts from an integral representation for the one-sided Laplace transform of a field quantity with respect to time of the following general form

$$G = (2\pi i)^{-1} \int_{-i\infty}^{i\infty} T \exp\left[-s\left(pd + \sum_{n=1}^{N} \gamma_n h_n\right)\right] \cdot (2\gamma_s)^{-1}\,dp \qquad \text{(A1)}$$

In (A1),

$$\gamma_n = (1/c_n^2 - p^2)^{1/2} \quad \text{with } (\ldots)^{1/2} \geq 0 \quad \text{along } \mathrm{Re}(p) = 0 \qquad \text{(A2)}$$

denotes the propagation coefficient of a wave propagating in the domain D_n and c_n is its speed of propagation, d is the "horizontal" distance from the source to the observer and h_n is the "vertical" path length of the trajectory that the wave has traversed in D_n. Hence, the exponential function in (A1) represents the propagation factor of the disturbance along the specified trajectory. The factor T in (A1) is algebraic in p and accounts for the transfer of the wave motion across the interfaces of the configuration (reflection and transmission); it contains $\gamma_1, \ldots, \gamma_N$ and the medium parameters. Finally, γ_s is the propagation coefficient in the medium where the source is located.

The main step in the modified Cagniard technique consists of properly deforming the path of integration in the right-hand side of (A1). To this end, we continue the integrand analytically into the

complex p plane, away from the imaginary axis, such that $\mathrm{Re}(\gamma_n) \geq 0$ in the entire part of the p plane into which the path of integration is deformable. This implies that branch cuts are introduced at $\mathrm{Im}(p) = 0$, $1/c_n \leq |\mathrm{Re}(p)| < \infty$ for all $n = 1, \ldots, N$. The deformed path of integration (modified Cagniard contour) is now chosen such that the propagation factor becomes of the form $\exp(-s\tau)$, where s is the (real and positive) Laplace-transform variable and τ is a real variable of integration (later to be identified with time). At infinity, supplementing circular arcs join the two paths. The contribution from these arcs vanishes provided that the modified path is located in $\mathrm{Re}(p) > 0$ and that the algebraic factors in the integrand in (A1) go to zero at infinity. In the applications that we consider, the latter condition is always satisfied. If the integrand has poles in the domain bounded by the original path of integration $\mathrm{Re}(p) = 0$, the modified Cagniard contour, and the circular arcs at infinity, their contribution should be properly taken into account. The modified Cagniard contour is not allowed to intersect one of the branch cuts introduced above. If it would be tempted to do so, it has to be supplemented by a loop integral around the relevant branch cut.

The equation satisfied by the modified Cagniard contour(s) is found as

$$\begin{aligned} \mathrm{Re}\Big(pd + \sum_{n=1}^{N} \gamma_n h_n\Big) &= \tau \\ \mathrm{Im}\Big(pd + \sum_{n=1}^{N} \gamma_n h_n\Big) &= 0 \end{aligned} \tag{A3}$$

Since γ_n is real and positive when $-1/c_n < \mathrm{Re}(p) < 1/c_n$, $\mathrm{Im}(p) = 0$, (A3) is certainly satisfied if

$$-\min(1/c_1, \ldots, 1/c_N) < \mathrm{Re}(p) < \min(1/c_1, \ldots, 1/c_N), \quad \mathrm{Im}(p) = 0 \tag{A4}$$

Note that if for one of the values of n we have $h_n = 0$, the restriction pertaining to the corresponding c_n in (A4) drops. Further, (A3) is satisfied along a certain path in the complex p plane that is located symmetrically with respect to the real p axis (because Schwarz's reflection principle applies to the left-hand side of (A3)) and goes to infinity. Hence, the latter contour and (parts of) (A4) are possible candidates for modified Cagniard contours.

First, we investigate the path in the complex p plane that goes to infinity. This part of the modified Cagniard contour corresponds to a body wave. Let

$$p = p^{\mathrm{BW}}(\tau) \quad \text{with } T^{\mathrm{BW}} \leq \tau < \infty \tag{A5}$$

denote its parametric representation in the first quadrant of the complex p plane, then the total path consists of $p = p^{\mathrm{BW}}$ and $p = p^{\mathrm{BW}*}$, where $*$ denotes the complex conjugate. The lower limit T^{BW} of τ in (A5) is the arrival time of the relevant body wave. This value is reached at the point of intersection of (A5) with the real p axis, where the minimum value of τ leads to an infinitely large value of $\partial_\tau p^{\mathrm{BW}}$. By differentiating (A3) with respect to τ, we obtain

$$\partial_\tau p^{\mathrm{BW}} = 1 \Big/ \Big[d - \sum_{n=1}^{N} (p^{\mathrm{BW}}/\gamma_n) h_n \Big] \tag{A6}$$

Let $\theta_1, \ldots, \theta_N$ be angles that are mutually related through Snell's law of refraction; then

$$p = (1/c_1)\sin(\theta_1) = \ldots = (1/c_N)\sin(\theta_N) \tag{A7}$$

makes the denominator of the right-hand side of (A6) vanish provided that

$$d - \sum_{n=1}^{N} h_n \tan(\theta_n) = 0 \tag{A8}$$

Substitution of (A7) in (A3) yields

$$T^{\mathrm{BW}} = \sum_{n=1}^{N} \frac{h_n}{c_n \cos(\theta_n)} \tag{A9}$$

which is the total travel time for a disturbance to propagate from the source to the point of observation along a trajectory that is in accordance with Fermat's principle (Figure 12).

If all terms in the summation of the left-hand side of (A3) are present (i.e., if none of the values $h_1, \ldots, h_N$ is zero), the condition (A7) ensures that $p = p^{\mathrm{BW}}$ intersects the real p axis between $p = 0$ and $\mathrm{Re}(p) = \min(1/c_1, \ldots, 1/c_N)$, $\mathrm{Im}(p) = 0$. In this case, the integral along $\mathrm{Re}(p) = 0$ equals the integral along $p = p^{\mathrm{BW}}$ and $p = p^{\mathrm{BW}*}$ plus contributions from possible poles. Then, we have

$$G = G^{\mathrm{BW}} + \text{contribution from poles} \tag{A10}$$

where, using Schwarz's reflection principle, G^{BW} is from (A1) obtained as

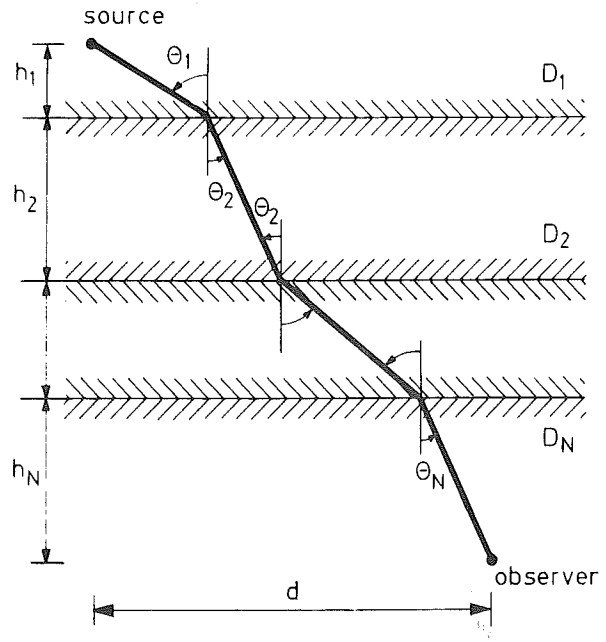

Fig. 12. Trajectory of a body wave in accordance with Fermat's principle.

$$G^{BW} = (1/\pi)\,\mathrm{Im}\left[\int_{T^{BW}}^{\infty} \exp(-s\tau)\,T(2\gamma_s)^{-1}\partial_\tau p^{BW}\,d\tau\right] \tag{A11}$$

Let us now consider the case that one of the values $h_1, \ldots, h_N$, h_M say, is zero. Then, no term corresponding to γ_M is present in (A3) and the situation may arise that, due to the presence of γ_M in the expression for T, an additional loop integral along the branch cut of γ_M must be included in order to apply Cauchy's theorem. The extra integral is needed if $p = p^{BW}$ intersects the real p axis at a point for which $\mathrm{Re}(p) > 1/c_M$, $\mathrm{Im}(p) = 0$. Obviously, this can only happen if $1/c_M < \min(1/c_1, \ldots, 1/c_{M-1}, 1/c_{M+1}, \ldots, 1/c_N)$. The relevant part of the modified Cagniard contour corresponds to a lateral wave. Let

$$p = p^{LW}(\tau) \quad \text{with } T^{LW} \le \tau \le T^{BW} \tag{A12}$$

denote its parametric representation in the first quadrant of the complex p plane, then the lateral-wave part of the modified Cagniard contour consists of $p = p^{LW}$ and $p = p^{LW*}$. The lower limit T^{LW} of τ in (A12) is the arrival time of the relevant lateral wave. This value is reached at $p = 1/c_M$. Substitution of this value in (A3) yields

$$T^{LW} = d/c_M + \sum_{n=1}^{M-1} (1/c_n^2 - 1/c_M^2)^{1/2} h_n + \sum_{n=M+1}^{N} (1/c_n^2 - 1/c_M^2)^{1/2} h_n \tag{A13}$$

where the square roots are all real and positive. In case the extra loop integral is needed, the integral along $\mathrm{Re}(p) = 0$ equals the integral along $p = p^{LW}$, $p = p^{LW*}$, $p = p^{BW}$, and $p = p^{BW*}$ plus contributions from possible poles. Then, we have

$$G = G^{LW} + G^{BW} + \text{contribution from poles} \tag{A14}$$

where, using Schwarz's reflection principle, G^{LW} is from (A1) obtained as

$$G^{LW} = (1/\pi)\,\mathrm{Im}\left[\int_{T^{LW}}^{T^{BW}} \exp(-s\tau)\,T(2\gamma_s)^{-1}\partial_\tau p^{LW}\,d\tau\right] \tag{A15}$$

while G^{BW} is given by (A11).

In case only a single term is present in the summation on the left-hand side of (A3), analytic expressions for the right-hand sides of (A5) and (A12) can be obtained. If more than a single term is present in the summation on the left-hand side of (A3), no simple analytic relationships exist and the right-hand sides of (A5) and (A12) will have to be determined with the aid of numerical techniques. In most cases, these are of an iterative nature and hence, they can be speeded up by choosing the starting value judiciously. Now, the values $p = P^{BW}$ and $p = P^{LW}$ obtained from the equation

$$pd + (1/C^2 - p^2)^{1/2} H = \tau \tag{A16}$$

where H and C are chosen such that (A16) approximates (A3), can serve as such. In (A16), we select the values of H and C in such a way that (A16) coincides with (A3) as $|p| \to \infty$ and at $p = 0$. From

$$p^{BW} \simeq \tau \Big/ \left(d - i\sum_{n=1}^{N} h_n\right), \quad \text{as } \tau \to \infty \tag{A17}$$

and

$$P^{BW} \simeq \tau/(d - iH), \quad \text{as } \tau \to \infty \tag{A18}$$

it follows that

$$H = \sum_{n=1}^{N} h_n \tag{A19}$$

while the conditions

$$p^{BW} = 0 \quad \text{at } \tau = \sum_{n=1}^{N} (h_n/c_n) \tag{A20}$$

and

$$P^{BW} = 0 \quad \text{at } \tau = H/C \tag{A21}$$

lead to

$$1/C = \left[\sum_{n=1}^{N} (h_n/c_n)\right] \Big/ H = \left[\sum_{n=1}^{N} (h_n/c_n)\right] \Big/ \left(\sum_{n=1}^{N} h_n\right) \tag{A22}$$

Solving (A16), the starting value P^{BW} of p^{BW} in the iteration process is then given by

$$P^{BW} = \frac{d}{d^2 + H^2}\tau + \frac{iH}{d^2 + H^2}\left[\tau^2 - (d^2 + H^2)/C^2\right]^{1/2}$$

$$\text{when } (d^2 + H^2)^{1/2}/C < \tau < \infty \tag{A23}$$

and the starting value P^{LW} of p^{LW} by

$$P^{LW} = \frac{d}{d^2 + H^2}\tau - \frac{H}{d^2 + H^2}\left[(d^2 + H^2)/C^2 - \tau^2\right]^{1/2}$$

$$\text{when } H/C < \tau < (d^2 + H^2)^{1/2}/C \tag{A24}$$

Note that the point of intersection (A7) of $p = p^{BW}$ with the real p axis does not coincide with the point of intersection of $p = P^{BW}$ as given by (A23) with the real p axis.

Figure 13 shows a number of modified Cagniard contours that have been used to evaluate the numerical results presented in Figures 4–11.

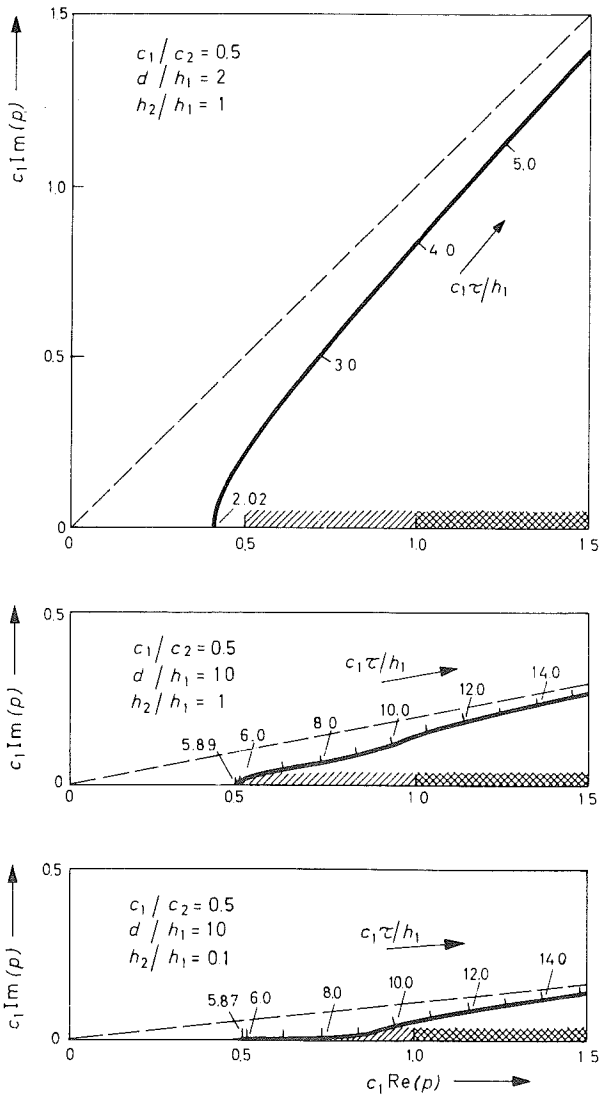

Fig. 13. Modified Cagniard contours that have been used to evaluate the numerical results presented in Figures 4–11.

Acknowledgments. This paper is dedicated to Professor H. Bremmer on the occasion of his 75th birthday. The author wishes to thank P. M. van den Berg, Laboratory of Electromagnetic Research, Delft University of Technology, for computing the numerical results and for helpful discussions.

REFERENCES

Achenbach, J. (1973), *Wave Propagation in Elastic Solids*, pp. 298–309, North-Holland, Amsterdam.

Baum, C. E. (1976*a*), The singularity expansion method, in *Transient Electromagnetic Fields*, edited by L. B. Felsen, pp. 129–179, Springer, New York.

Baum, C. E. (1976*b*), Emerging technology for transient and broad-band analysis and synthesis of antennas and scatterers, *Proc. IEEE, 64*(11), 1598–1616.

Burridge, R. (1971), Lamb's problem for an anisotropic half-space, *Quart. J. Mech. Appl. Math., 24*, Pt. 1, 81–98.

Cagniard, L. (1939), *Réflexion et Réfraction des Ondes Séismiques Progressives*, 255 pp., Gauthier-Villars, Paris.

Cagniard, L. (1962), *Reflection and Refraction of Progressive Seismic Waves*, 282 pp., McGraw-Hill, New York. (Translation and revision of *Cagniard* [1939] by E. A. Flinn and C. H. Dix.)

de Hoop, A. T. (1958), Representation theorems for the displacement in an elastic solid and their application to elastodynamic diffraction theory, pp. 32–78, thesis, Delft University of Technology, Delft, The Netherlands.

de Hoop, A. T. (1960), A modification of Cagniard's method for solving seismic pulse problems, *Appl. Sci. Res., B8*, 349–356.

de Hoop, A. T. (1961), Theoretical determination of the surface motion of a uniform elastic half-space produced by a dilatational impulsive, point source, in *La Propagation des Ébranlements dans les Milieux Hétérogènes*, Coll. No. 111, Centre National de la Recherche Scientifique, pp. 21–32, CNRS, Paris.

de Hoop, A. T., and H. J. Frankena (1960), Radiation of pulses generated by a vertical electric dipole above a plane, nonconducting earth, *Appl. Sci. Res., B8*, 369–377.

Felsen, L. B., and N. Marcuvitz (1973), *Radiation and Scattering of Waves*, pp. 523–527, Prentice-Hall, Englewood Cliffs, New Jersey.

Frankena, H. J. (1960), Transient phenomena associated with Sommerfeld's horizontal dipole problem, *Appl. Sci. Res., B8*, 357–368.

Johnson, L. R. (1974), Green's function for Lamb's problem, *Geophys. J. Roy. Astron. Soc., 37*, 99–131.

Langenberg, K. J. (1974), The transient response of a dielectric layer, *Appl. Phys., 3*, 179–188.

Suh, S. L., W. Goldsmith, J. L. Sackman, and R. L. Taylor (1974), Impact on a transversely anisotropic half-space, *Int. J. Rock Mech. Min. Sci. Geomech. Abstr., 11*, 413–421.

Van der Pol, B., and H. Bremmer (1950), *Operational Calculus Based on the Two-sided Laplace Integral*, pp. 7–21, Cambridge University Press, London.

Widder, D. V. (1946), *The Laplace Transform*, p. 63, Princeton University Press, Princeton, New Jersey.